

# Pairing correlations of cold fermionic gases at overflow from a narrow to a wide harmonic trap

A. Pastore,<sup>1,\*</sup> P. Schuck,<sup>2,3</sup> M. Urban,<sup>2</sup> X. Viñas,<sup>4</sup> and J. Margueron<sup>2,5</sup>

<sup>1</sup>*Institut d'Astronomie et d'Astrophysique, CP 226,  
Université Libre de Bruxelles, B-1050 Bruxelles, Belgium*

<sup>2</sup>*Institut de Physique Nucléaire, Université Paris-Sud, IN2P3-CNRS, F-91406 Orsay, France*

<sup>3</sup>*Laboratoire de Physique et de Modélisation des Milieux Condensés, CNRS et Université Joseph Fourier,  
UMR5493, 25 Av. des Martyrs, BP 166, F-38042 Grenoble Cedex 9, France*

<sup>4</sup>*Departament de estructura i Constituents de la Matèria and Institut de Ciències del Cosmos,  
Facultat de Física, Universitat de Barcelona, Diagonal 647, E-08028 Barcelona, Spain*

<sup>5</sup>*Université de Lyon, Institut de Physique Nucléaire de Lyon, IN2P3-CNRS, F-69622 Villeurbanne, France*  
(Dated: June 29, 2021)

Within the context of Hartree-Fock-Bogoliubov theory, we study the behavior of superfluid Fermi systems when they pass from a small to a large container. Such systems can be now realized thanks to recent progress in experimental techniques. It will allow to better understand pairing properties at overflow and in general in rapidly varying external potentials.

PACS numbers: 32.80.Pj, 05.30.Fk

## I. INTRODUCTION

Finite systems of superfluid fermions exist in different situations such as, for example, traps of cold atoms, atomic nuclei, or small metallic clusters. All these different systems can be treated using the same many-body theory, namely the Bogoliubov-de Gennes (BdG) theory [1, 2], in nuclear physics usually called Hartree-Fock-Bogoliubov (HFB) theory, valid also for finite range pairing forces [3]. In a recent series of articles [4, 5], the authors have studied the behavior of different systems of fermions once their Fermi levels reach the edge of a finite container, *i.e.*, either the fluid overflows into the continuum or it pours into another container of much larger dimension. Such a situation has been experimentally observed in systems of cold bosonic atoms [6, 7] and it should also be possible to use it for fermionic atoms [8]. This phenomenon is supposed to be realized also in the inner crust of neutron stars (NS) in the transition region between the outer and the inner crust [9]. Going from the outer layer to the inner one, *i.e.* from low to high density regions, the formation of very neutron rich nuclei is favored by the NS environment and eventually they can reach the neutron drip line. Further increasing the density, the neutrons can not be bound anymore and we observe the coexistence of a lattice of nuclei immersed in a diluted neutron gas. This situation often is mimicked by the use of Wigner-Seitz (WS) cell [10, 11], where the single particle potential has a pocket, representing the nucleus, embedded in a large container. Understanding the role of pairing correlations in these systems is thus important and will help us to get general insight into the behavior of superfluid Fermi systems in rapidly varying external potentials.

The aim of the present article is to give considerably more details and to extend the study of [4, 5], considering cold atoms as a relatively simple bench mark system. In cold atom systems the interparticle distance is by orders of magnitude larger than the range of the force between atoms, so that the latter is usually replaced by a contact interaction with a well-known regularisation scheme [12, 13]. The systems considered in [4, 5] were treated not with the BdG (HFB) theory but using the BCS approximation in which non-diagonal matrix elements of the gap are neglected. These calculations were performed using a bare contact force with a cut-off. However, the BCS approximation fails in the case of cold atoms when a contact force with the usual regularisation procedure is used. We have checked this numerically but it may also become clear from the fact that the BCS wave function, contrarily to the HFB-one, has not the correct asymptotic behavior when the relative distance between the two particles goes to zero. It is, therefore, an important issue to see by how much the conclusions of [4, 5] are altered in using the correct BdG(HFB) approach. We will see that qualitatively the quench of the gap at overflow persists. However, we will have to correct one conclusion drawn from the BCS approximation concerning the spatial behavior of the gap in the interior of the trap where the BCS solution does not behave as the BdG(HFB) one. We also will present new features as, for instance, the spatial behavior of the wave functions before and after the spill which will give more insight into the fact why the gap becomes quenched passing the drip.

The article is organized as follows: in Sec.II we present the HFB equations we used in our calculations and we also discuss the properties of the adopted pairing interaction. In Sec.III, we present our numerical results and finally in Sec.IV, we give our conclusions.

---

\*Electronic address: apastore@ulb.ac.be

## II. THE HARTREE-FOCK BOGOLIUBOV OR BOGOLIUBOV-DE GENNES APPROACH

To discuss the pairing properties of a system of cold atoms, we adopt the mean-field description based on the HFB equations [3] or, equivalently, the BdG equations [2]. The difference between both methods is marginal: the BdG equations are tailored for zero range forces, *i.e.* local pairing fields, whereas nuclear forces are in general finite ranged and, thus, also the pairing field becomes non-local demanding the more general HFB scheme. Using an effective zero range interaction, we can express the HFB (BdG) equations in  $r$ -space as [13, 14]

$$\begin{aligned} [H_0 + W(\mathbf{R})]u_\alpha(\mathbf{R}) + \Delta(\mathbf{R})v_\alpha(\mathbf{R}) &= E_\alpha u_\alpha(\mathbf{R}) \\ \Delta(\mathbf{R})u_\alpha(\mathbf{R}) - [H_0 + W(\mathbf{R})]v_\alpha(\mathbf{R}) &= E_\alpha v_\alpha(\mathbf{R}). \end{aligned} \quad (1)$$

We have used  $\alpha = \{nls\}$  as a short-hand notation for the quantum numbers of the system; since we have chosen a system with perfect symmetry between states of opposite spin  $N/2 = N_\uparrow = N_\downarrow$ , for brevity, we can simply drop the spin quantum number  $s$ . In Eqs.(1),  $H_0 = T + U(R) - \mu$ ;  $T = -\hbar^2 \nabla^2 / 2m$  is the kinetic energy,  $\mu$  is the chemical potential and  $U(R)$  is the external trap potential.  $W(\mathbf{R})$  is the Hartree potential. We will neglect it in this paper, since it is not essential for our following considerations. Let us again point out that the present work may have generic character for all situations where a superfluid Fermi liquid pours from a narrow to a much wider container. We will consider quite large systems where shell effects are not very important, but we briefly will also touch smaller ones. As it is known, in the case of nuclei the superfluid mechanism can be strongly influenced by the underlying level structure [15, 16]

In the present article, following the discussion of Refs. [4, 5] we have adopted a spherical double-harmonic potential of the form

$$U(R) = \begin{cases} \frac{1}{2}m\omega_1^2 R^2 & \text{if } R < R_0, \\ \frac{1}{2}m[\omega_2^2 R^2 + (\omega_1^2 - \omega_2^2)R_0^2] & \text{elsewhere.} \end{cases} \quad (2)$$

From now on, we will use the system of units of the trap, *i.e.*,  $\hbar = \omega_1 = m = 1$ . In other words, energies are measured in units of  $\hbar\omega_1$ , lengths in units of the harmonic oscillator length  $\sqrt{\hbar/m\omega_1}$ , etc. We choose  $R_0 = \sqrt{50} \approx 7.1$  in these units. In Fig.1, we show the radial profile of the external trap. We observe that according to the ratio  $r = \omega_2/\omega_1$ , we can define different configurations. Going from  $r = 1$  to  $r = 0.1$ , we create an overflow point at  $U(R_0)=25$ .

The HFB equations (1) are solved in the basis of the eigenfunctions of the potential (2) up to a maximum energy  $E_C$ . A similar method has been already described in ref [17] for the nuclear case.

The pairing potential  $\Delta(R)$  originates from a contact pairing interaction. As already discussed in Ref. [18], the contact interaction presents an ultraviolet divergence. To avoid such a problem we can either fix the phase space

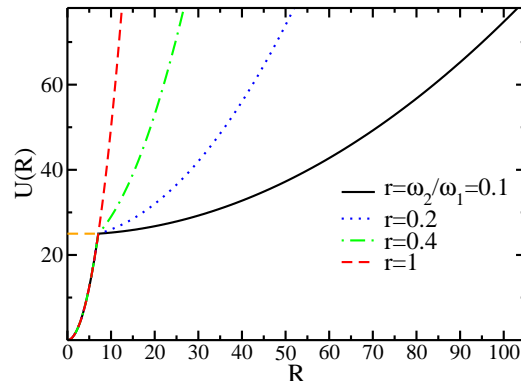


FIG. 1: (Colors online) The different trapping potentials  $U(R)$  used in this work, as defined in Eq.(2). The ratio among the two harmonic potentials is  $r = \omega_1/\omega_2 = 0.1, 0.2, 0.4, 1$ .  $U$  and  $R$  are in trap units, *i.e.*, in units of  $\hbar\omega_1$  and  $\sqrt{\hbar/m\omega_1}$ , respectively [cf. text below Eq.(2)].

where we perform our calculations by introducing a cut-off [4, 5, 19] or we can identify the nature of the divergent term and regularize the interaction. The latter procedure has been suggested in Ref. [18] and it will be the method followed in the present article.

Following Ref. [13], we write the gap equation with an effective contact pairing interaction as

$$\Delta(R) = g_{\text{eff}}(r) \sum_{nl} \frac{2l+1}{4\pi} u_{nl}(R)v_{nl}(R). \quad (3)$$

Since we work in a finite basis,  $n$  and  $l$  cannot exceed maximum values defined by the cut-off energy  $E_C$ . However, the results will not depend on the choice of  $E_C$  if it is sufficiently large. This cut-off should not be confused with the one adopted in Refs. [4, 5], since in that case the authors have used a bare contact force  $g$ , while here we use an effective contact force  $g_{\text{eff}}$  which compensates the cut-off dependence. This effective interaction reads

$$\frac{1}{g_{\text{eff}}} = \frac{1}{g} + \frac{1}{2\pi^2} \left[ \frac{k_F(R)}{2} \log \frac{k_C(R) + k_F(R)}{k_C(R) - k_F(R)} - k_C(R) \right], \quad (4)$$

where  $k_F(R) = \sqrt{2(\mu - U(R))}$  is the local Fermi momentum and  $k_C(R) = \sqrt{2(E_C - U(R))}$  is the momentum corresponding to the cut-off.

The coupling constant  $g$  is related to the atom-atom scattering length  $a$  by  $g = 4\pi a$ . Unless otherwise stated, we will use  $g = -1.56$ , corresponding to  $k_F a = -0.88$  at the center of the trap for  $\mu = 25$ . Those numbers fall well into the domain what is attainable with the help of Feshbach resonances in real cold atom systems. Our study will, therefore, provide a definite experimental prediction.

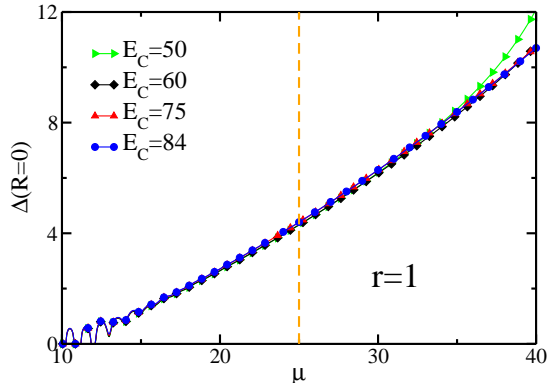


FIG. 2: (Colors online) Evolution of the pairing field at the center of the trap  $\Delta(R=0)$  as a function of the chemical potential  $\mu$  in the trap configuration  $r = \omega_2/\omega_1 = 1$  for different cut-off values  $E_C$  for  $g=-1.56$ . All quantities are expressed in trap units [cf. text below Eq.(2)].

As already discussed in ref. [13], we have to check that our calculations are fully converged, *i.e.*, that they do not depend on the given value of  $E_C$ .

In Fig.2, we show for the trap configuration the evolution of the pairing field at the center of the trap  $\Delta(R=0)$  as a function of the chemical potential and different values of the cut-off  $E_C$ . The calculations are well converged for the choice  $E_C = 84$  around small values of the chemical potential, and in particular for the region around  $\mu = 25$ , where we have the drip point. See Fig.1. The result is in agreement with the conclusions of Ref. [13]. At higher values of the chemical potential, we notice that the adopted value of  $E_C$  is not very adequate and a larger value would be preferable. As already mentioned in the introduction, we again want to stress here that the outlined theoretical scheme can in no way be approximated by the simple BCS approach of [4, 5] where the off-diagonal elements of the gap are neglected.

In order to show the typical system sizes we are dealing with in this work, we display in Fig.3 the number of atoms in the trap as a function of the chemical potential  $\mu$  for two trap configurations. Please, notice the practically exponential increase of particle numbers, once the large container starts being populated.

### III. RESULTS

Having checked the numerical accuracy that we can achieve in our calculation, we can finally present our results.

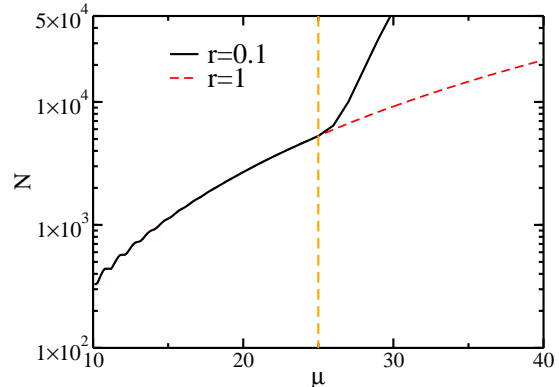


FIG. 3: (Colors online) Number of particles as a function of the chemical potential (in units of  $\hbar\omega_1$ ) for two trap configurations.

#### A. HFB

One of the most prominent indicators of superfluidity is the presence of a gap in the level density. It may not be very easy to measure it in cold atom systems, but in metallic superconductors the level density around the Fermi level is measured routinely [20]. May be, if one day a metallic grain device can be constructed with small and wide container geometry as discussed here, it may be possible to measure the level density across the drip point. In any case, we will discuss the result of our calculation for the superfluid level density. A simplified version of the level density for the BCS case has been also presented in ref. [21]. Here, we give the full expression

$$g(E) = 2 \sum_{E_{nl} > 0} (2l+1) [ \|v_{nl}\|^2 \delta(E + E_{nl}) + \|u_{nl}\|^2 \delta(E - E_{nl}) ] \quad (5)$$

where  $E$  is the energy measured from the chemical potential  $\mu$ ,  $E_{nl}$  is the HFB quasi-particle (qp) energy, and  $\|v_{nl}\|$ ,  $\|u_{nl}\|$  denote the norms of the wave functions  $v_{nl}$  and  $u_{nl}$ , respectively. Results for various system parameters are shown in Fig. 4. In Fig.4(a)-(b) we show the level density for  $\mu$ -values slightly below and slightly above the drip point, respectively. For the ratio  $r = 0.1$ , we clearly see a break down of the gapped window when passing from below to above the drip. Also shown is the level density without pairing for better comparison (panels 4(c)-(d)). Actually it is easier to represent the lowest qp energy as a function of the chemical potential, since the gap in the spectrum is essentially given by two times the lowest qp energy. This is shown in Fig. 5. We clearly see that there is a strong break down of the gap passing through the drip point at  $\mu = 25$ . This drop is the more pronounced, the smaller the ratio  $r$ . For  $r = 0.1$ , the gap

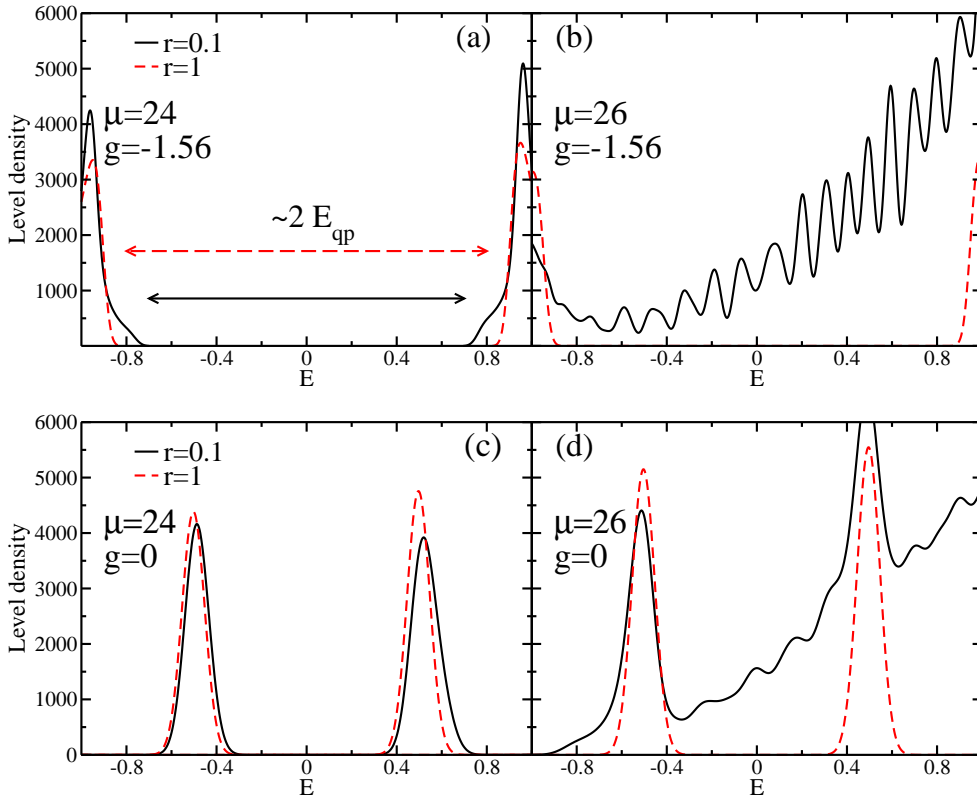


FIG. 4: (Color online) Level density as given in Eq.(5) for the two extreme traps as shown in Fig.1. On the left panels the calculations are done at  $\mu = 24$ , while on the right panels  $\mu = 26$ . In panels (a)-(b) we show the level densities from HFB calculations and in (c)-(d) the ones without pairing. The discrete level densities are folded with gaussians of width  $\sigma = 0.05$  for the case with pairing (panels a and b) and  $\sigma = 0.1$  for the case without pairing (panels c and d). All quantities are expressed in trap units.

drops practically to zero after the drip. It is interesting to note that the decrease of the gap actually starts already *before* reaching the drip point and precisely at overflow the gap is already down by an important factor. This result is quite well in agreement with the qualitative prediction given in [4] where, however, the more crude BCS approximation was used. We also can see from Fig. 5 that once the chemical potential is well below the drip point, quite prominent shell fluctuations start to develop. Shell fluctuations will also appear in other quantities and further be discussed in section III B. It is rather easy to understand why there is this drop of the spectral gap and eventually other pairing quantities across the overflow point. Since the individual wave functions after the threshold have a much wider extension, still being normalized to unity, their overlap in the matrix elements of the pairing force becomes much smaller. What, nevertheless, is surprising, is the sharpness of the transition displayed in Fig. 5. Numerically, we cannot handle still smaller values of  $r$  than  $r = 0.1$ . However, from Fig.5, it becomes quite clear that in the limit  $r \rightarrow 0$ , *i.e.*, for a

truly finite potential, the lowest quasiparticle and, thus, the gap will become very close to zero, once the chemical potential  $\mu$  reaches the top of the finite container.

In order to make the influence of pairing more pronounced, we repeated the calculation using different values of the coupling constant  $g$ . In Fig. 6, we present a zoom on the level density in the energy interval  $E \in [-2.5, +0.5]$  (where the energy is measured from the chemical potential  $\mu$ ) for four values of the coupling constant  $g$  as indicated in the panels. In each panel, we also give the level density in LDA (broken lines), see Sect.III B. The underlying basis is the same for the four different calculations and we just change the value of the coupling constant  $g$ . We notice that for a range of coupling constants  $g \lesssim 2$ , the pairing correlations are not strong enough to create a gap in the level density on the scale of the figure. Only, once we increase the coupling constant by a factor of four, we can observe the appearance of a tiny gap in the LDA level density around  $E = 0$ . Quantally (*i.e.*, within HFB), there are only discrete levels and it is very difficult to pin down any opening of

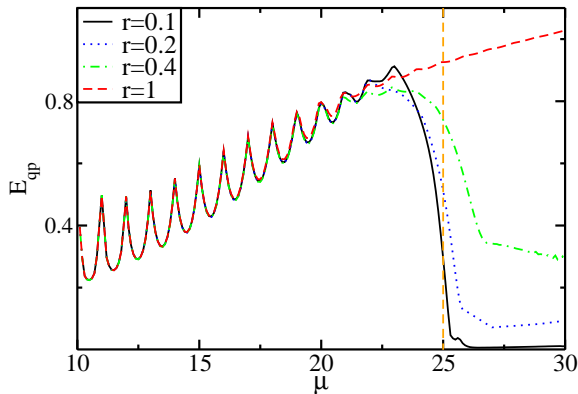


FIG. 5: (Colors online) Evolution of the lowest quasi-particle energies as a function of the chemical potential (both in units of  $\hbar\omega_1$ ) for various potential configurations.

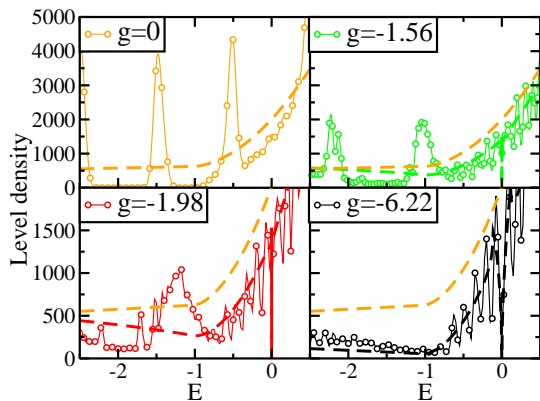


FIG. 6: (Colors online) Level density as given in Eq.(5) for the trap configuration  $r = \omega_2/\omega_1 = 0.1$  at  $\mu = 26$  and four different values of coupling constant. On the same figure we represent with dashed line and same color code the results obtained using the LDA approximation. All quantities are expressed in trap units.

a gap in this case. For comparison, we have also represented the case without pairing obtained with LDA in all panels (yellow broken lines). We not only see the (narrow) window at  $E = 0$ , but remark that even globally the level density is suppressed in the superfluid case as seen for instance for  $g = -6.22$  (lower right panel of Fig.6). This stems from the fact that for this increased pairing force, the gap in the narrow part of the potential is so strong that it still influences the level density far from the Fermi energy (*i.e.*, far from  $E = 0$ ).

We have also analyzed the diagonal matrix elements of

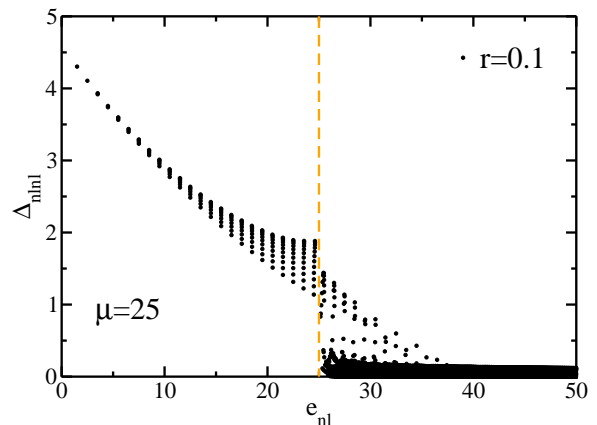
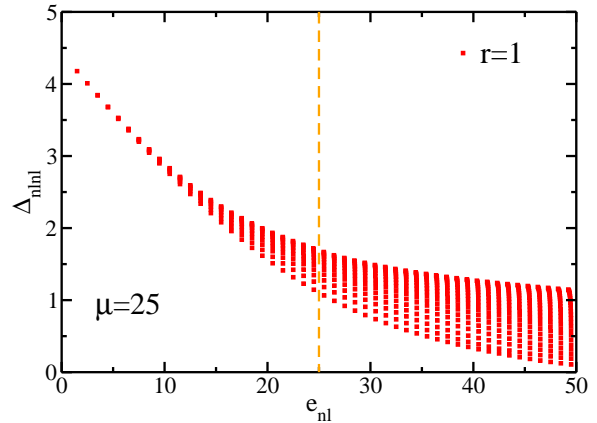


FIG. 7: (Colors online) Diagonal matrix elements of the pairing field,  $\Delta_{nlnl}$ , as a function of the energy of the basis state  $n$  at  $\mu = 25$  for two different configurations ( $\Delta_{nlnl}$ ,  $e_{nl}$ , and  $\mu$  in units of  $\hbar\omega_1$ ). In the upper panel we use the trap configuration  $r = 1$ , while in lower panel  $r = 0.1$ .

the gap (as they are used in the BCS approximation, see Refs. [4, 5]) as a function of the single particle energies as they are given in our basis, see Fig. 7. We observe a clear drop of most of those gap values beyond the overflow point at  $\mu = 25$  in the case  $r = 0.1$ . However, what is interesting is the fact that some of those gaps in the region  $\mu > 25$  apparently still belong to the narrow container. As already discussed in the nuclear case [15, 16], those gaps correspond to 'resonances' of the narrow container in the 'continuum' (actually levels are, of course, still discrete above the drip point but very dense, *i.e.* one may consider it as a quasi-continuum). Those resonances correspond in the nuclear case to states trapped by the centrifugal barrier of the narrow container. We suppose that the same features are at work in our present case.

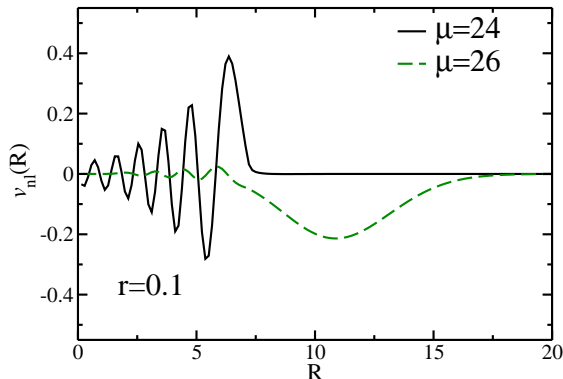


FIG. 8: (Colors online) The radial spinor  $v_{nl}(R)$  as defined in Eq.1 corresponding to the lowest quasi-particle as shown in Fig.5 for the trap configuration  $r = 0.1$ . The solid line refers to the case  $\mu = 24$ , while the dashed line to the case  $\mu = 26$ . All quantities are expressed in trap units.

It is also interesting to study the behavior of the wave functions  $v(R)$  ( $u(R)$  is similar). In Fig. 8, we show  $v_{nl}(R)$  corresponding to the lowest quasi-particle energy for the case of  $r = \omega_2/\omega_1 = 0.1$  for two values of the chemical potential  $\mu = 24$  and  $\mu = 26$ . We see that the behavior of the wave function for the case of  $\mu = 24$  is quite similar to the case presented by Baranov [22] and by Bruun and Heiselberg [23], namely that the wave function is suppressed in the center of the trap (where  $\Delta(R)$  is large) and is mostly concentrated on the surface of the gas..

The situation changes quite significantly in the case of  $\mu = 26$ . The extension of the wave function is radically increased and spills far into the wide container with a large amplitude. Such an effect is, of course, expected but it is of interest to see it quantitatively. This behavior explains the small energy of the lowest quasiparticle energy after the overflow shown in Fig. 5.

## B. LDA

In cold atom systems, it is common use to solve the pairing problem in the homogeneous case and then to use the local-density approximation (LDA) [3], which amounts to replacing  $\Delta$  by  $\Delta(R)$  and  $\mu$  by  $\mu(R) = \mu - U(R)$ . Usually this works quite well as has recently been discussed in detail in ref. [13]. So, let us see how LDA works in the present case.

Again the interesting quantity may be the level density in LDA. How to calculate the level density within LDA is demonstrated in [21] (but here we make use of the LDA version of Eq.(5) which is slightly more general than the one given in [21]). We show the results in Fig.6

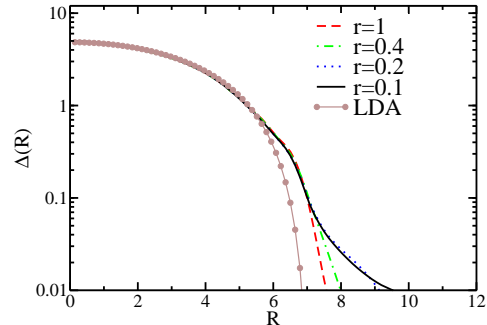


FIG. 9: (Colors online) Pairing field  $\Delta(R)$  calculated at  $\mu = 26$  for different trap configurations. The filled circles indicate the result obtained using the LDA for  $r = 0.1$ . All quantities are expressed in trap units.

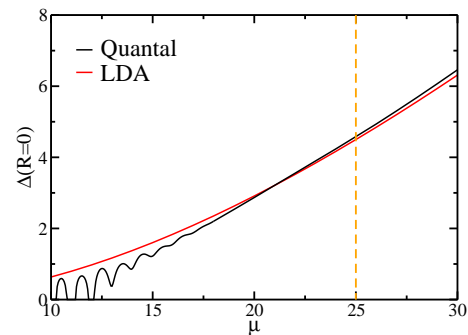


FIG. 10: (Colors online) Comparing the quantal and LDA calculations of pairing field  $\Delta(R = 0)$  as function of the chemical potential  $\mu$  (both in units of  $\hbar\omega_1$ ) for the trap configuration  $r = 0.1$ .

(broken lines). In this figure we display the LDA results using different values of the coupling constant  $g$  and fixed trap configuration  $r = \omega_2/\omega_1 = 0.1$ . The results are in good agreement with the quantal ones in the sense that the LDA is able to reproduce the average quantities thus passing through the peaks obtained in the HFB calculations. We also observe, as already mentioned, that the LDA level density always goes to zero at the Fermi energy (*i.e.*, at  $E = 0$ ) as it should be, but on the scale of the figure one only can notice a very small gap for the case of the increased pairing force  $g = -6.22$ .

In systems of cold atoms, one can measure the gap locally [24]. In Fig. 9, we show the local gap  $\Delta(R)$  as a function of position for the quantal case compared to LDA for the ratio  $r = 0.1$ . It is seen that at large radii, the LDA result drops too fast (as soon as  $\Delta(R)$  becomes smaller than the level spacing of the trap). Quantitatively, for expectation values, this may not be very relevant, how-

ever, because the logarithmic scale on the vertical axis in Fig. 9 makes the effect look more important than it is.

Let us now look at the maximum of the local gap, which is at the origin of the trap. In Fig.10 we show  $\Delta(R=0)$  as a function of  $\mu$  quantally and in LDA. We see that this quantity is monotonously and constantly rising, also across the drip point and that quantal and LDA results well agree on the high energy side (the very small disagreement likely is an effect of not 100% converged results as the chemical potential reaches higher values). This, however, is not in contradiction with the fact that the spectral gap is sharply dropping after the overflow as seen in Fig.5, since the spectral gap depends mainly on what happens at the surface of the system, see Fig.8. An important qualitative difference between the BCS prediction and the BdG-HFB approach can be seen on Figs. 9,10 . Whereas at overflow the BCS approximation entails a strong negative influence on what happens for the gap also at the center of the trap, this is not at all the case with the BdG-HFB, see, for instance, Fig. 9. On the contrary, as seen on Fig. 5 of [4], in the BCS case, the gap inside seems to disappear alongside with the disappearance of the gap outside, thus, invalidating the BCS approximation for this feature.

In principle other quantities may be of interest. For example how does the difference of energy per particle,  $\Delta E$  with and without pairing vary as a function of the chemical potential? The same question may be asked for the pairing energy, etc. However, the latter quantity diverges (as a function of  $E_C$ ) for the present contact interaction, only the total energy converges. On the other hand the (tiny) energy difference  $\Delta E$  comes as a result of the difference of two big numbers and the accuracy of our code did not allow us to obtain totally stable results. Thus, we do not present them here. However, our estimates are such that, *e.g.*, the drop of pairing correlations across the overflow, seen already for the level density and the lowest quasi particle energy, is confirmed also for the above mentioned difference of energies.

### C. Small particle number

One may think that the features outlined above for the double harmonic potential may change if in the narrow part of the potential are not several thousands but only several hundreds of particles reaching the drip, a situation which prevails, *e.g.*, in the nuclear case. Note that also in traps it is now possible to study systems with very small atom numbers [25]. We, therefore, show in Fig.11 again the lowest quasi particle energies as a function of  $\mu$  for a case where the overflow occurs at  $\mu = 12.25$  corresponding to an extension of the narrow part of the trap  $R_0 = 4.95$ , see Fig. 1. In Fig.12 the gap at the center is displayed as a function of  $\mu$ . A little unexpectedly the situation stays qualitatively similar to the cases shown in

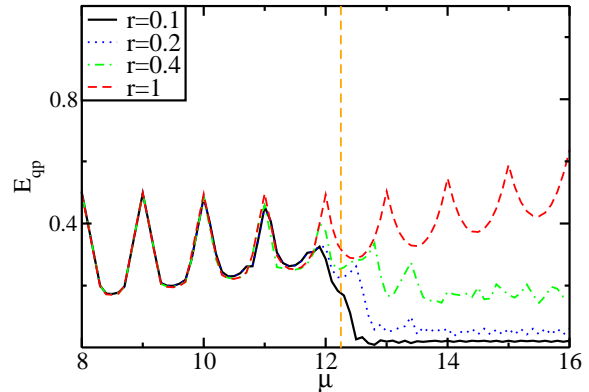


FIG. 11: (Colors online) Same as Fig.5, but for overflow at  $\mu = 12.25$  and  $R_0 = 4.95$  (in trap units). See text for more explanation.

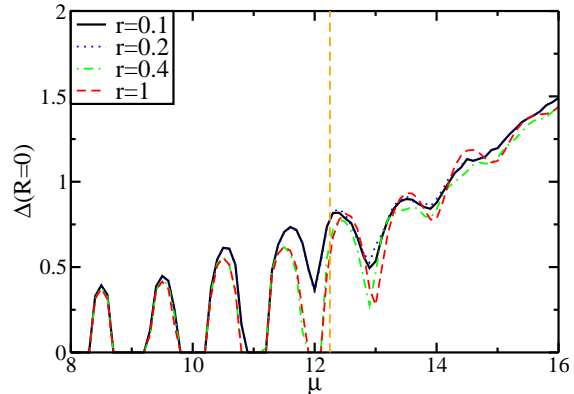


FIG. 12: (Colors online) Pairing field at the center of the trap  $\Delta(R=0)$  as a function of the chemical potential  $\mu$  (both in units of  $\hbar\omega_1$ ) for the same trap configuration as in Fig.11 and different ratios  $r$ .

Fig.5 and Fig.10, only the influence of the shell effects is now much stronger.

### D. Physical Consequences

As we mentioned already, in some systems the gap can directly be measured via the level density. It remains an open question whether for instance metallic grains can geometrically be tailored into such a double well configuration. In other systems, like nuclei and ultra small metallic grains the even-odd effect, directly related to the gap, can be extracted from experimental data [26]. As

we mentioned already, in nuclei with their quite small number of particles, the drop of pairing is strongly overshadowed by shell fluctuations. However, the tendency of reduced pairing correlations towards, for instance, the neutron drip is also clearly seen there from theoretical calculations [15, 16]. However, static gaps being interesting, the more spectacular expression of superconductivity and superfluidity comes from the dynamics, as for example collective modes or rotational motion, etc. One may be interested in situations where the linear response regime applies and, thus, only the configurations very close to the Fermi level are active. So, since the gap values drastically drop in the overflow regime, this will also affect the dynamics. For example, because of the reduced gap, pair breaking (at small but finite temperature) will occur much more frequently after the drip into the large container than before and, therefore, the collective flow will become more normal fluid like. To be more quantitative, let us discuss the situation of slow rotation [27, 28]. In this (and other) situation(s) it is not so much the absolute value of the spectral gap which plays a role but rather the ratio of the gap vs the average level spacing. In our case, this would mean to scale the gap to the frequencies  $\omega_i$ .  $\Delta/\omega > 1$  is the regime of irrotational flow, whereas  $\Delta/\omega < 1$  is the regime of rigid body motion. Of course around the drip it is difficult to say which of the two  $\omega$ 's to take.

It is interesting to notice that even with a rescaling of the lowest quasiparticle energy shown in Fig. 5, which roughly may be identified with the gap, the sharp drop across the drip point is still there, even though less pronounced. For example multiplying the case  $r = 0.1$  (black solid line) by a factor ten beyond  $\mu = 26$  will not reduce the break down by a large amount. Therefore, *e.g.*, the moment of inertia of a deformed slowly rotating trap would be much less close to its irrotational flow value after the drip than before. Even in an almost full finite container this would be the case, since the lowest quasiparticle energy, *i.e.*, implicitly the gap, is strongly reduced already before the top of the container is reached, see Fig. 5. This is an interesting and, may be, unexpected physical consequence of our study. It should apply equally to other dynamical quantities as the already mentioned collective modes, see, *e.g.*, Ref [29].

On the other hand, if the system enters the nonlinear regime where vortices are created, certainly, in the steady state configuration, the first appearing vortex will be centered at the origin where the gap is maximum independent of what happens around the Fermi surface.

#### IV. CONCLUSIONS

In this work, we enlarged and refined our previous study on superfluid Fermi systems at overflow. This means having a container which passes as a function of filling, *i.e.*, as a function of chemical potential abruptly

from a narrow to a wide container. The transition point is called the overflow or drip point. Our initial interest came from nuclear physics where such situations may be relevant for very neutron rich nuclei in the laboratory or for nuclei in the crust of neutron stars. There, as a function of the deepness in the crust, the nuclei may or may not be embedded in a gas of dripped superfluid neutrons. In this work we studied as a generic example the situation with cold atoms where a trapping potential of this kind had already been fabricated but for bosons. However, theoretical studies have also been performed with fermions [8]. Eventually, one may also arrange superconducting metallic grains geometrically and energetically in such a way that a double well with varying chemical potentials is created. In finite nuclei, the effects at the neutron drip is strongly overshadowed by shell fluctuations, but a clear average tendency of reduced pairing is also visible there [16].

The technical improvement compared to our earlier publications here is that we treat the cold atom situation with thousands of atoms not in the BCS approximation (*i.e.*, keeping only the diagonal elements of the gap) but rather with the BdG (HFB) approach which is more realistic and even absolutely necessary if one wants to use the standard renormalization method for the contact interaction where one replaces the bare interaction by the scattering length. We, indeed, found that the BCS approximation fails in the case of cold atoms when a contact force is used together with the usual regularisation scheme. In addition, the BCS approximation turns out to be inadequate for one of the conclusions advanced in [4], namely that the drop of pairing after the drip also entails a corresponding reduction of the gap in the center of the trap. On the contrary, as we show in this work, with the BdG-HFB approach, the gap at the center remains rather unaffected passing through the drip point in a monotonous way. On the other hand, we have seen that qualitatively the main conclusions with respect to our earlier BCS ones remain unchanged. This concerns, for instance, the finding that the spectral gaps drop surprisingly sharply across the overflow point and a strong reduction can already be seen before reaching the break point. In fact, in the limit where the wide container completely opens up, we reach the situation of a single finite potential well. We discussed that in this case, the spectral gap drops to zero when the chemical potential reaches the upper limit, the reduction of the gap starting already well before this limit is reached. We have shown that this effect is also present in the level density which in some systems may be a measurable quantity. We also investigated the wave functions of the lowest quasi-particle states and found that they are concentrated in the surface. This explains the drop of the gap after the drip as demonstrated with the calculation of the lowest quasi particle energy and, also, the level density before and after the overflow.

In Refs.[4, 5], we also studied the Thomas-Fermi (TF)

version of BCS using a cut off or a finite range interaction and obtained very good agreement with the corresponding quantal BCS results. An extension of TF to HFB or BdG is planned for the future.

It may be noticed that for cold atom systems, we give a definite experimental prediction in this work. We also discussed the influence of our finding on dynamic quantities like moment of inertia and other flow aspects.

### Acknowledgments

One of us (X.V.) acknowledges financial support from Spanish Consolider-Ingenio 2010 Programme CPAN

CSD2007-00042 and from Grants No.FIS2011-24154 MICINN and FEDER and No.2009SGR-1289 from Generalitat de Catalunya. We thank A. Polls for interesting discussions on recent theoretical progress in cold atom physics.

- 
- [1] J. Bardeen, L. N. Cooper, and J. R. Schrieffer, *Phys. Rev.* **108**, 1175 (1957).
- [2] P. G. De Gennes, *Superconductivity Of Metals And Alloys*, Advanced Book Classics (Advanced Book Program, Perseus Books, 1999), ISBN 9780738201016.
- [3] P. Ring and P. Schuck, *The Nuclear Many-Body Problem* (Springer-Verlag, 1980).
- [4] P. Schuck and X. Viñas, *Physical Review Letters* **107**, 205301 (2011).
- [5] P. Schuck and X. Viñas, in *50 Years of Nuclear BCS*, edited by W. S. P. C. s. R.A.BrogliA and V.Zelevinsky Editors (2012), p. 212.
- [6] D. M. Stamper-Kurn, M. R. Andrews, A. P. Chikkatur, S. Inouye, H.-J. Miesner, J. Stenger, and W. Ketterle, *Phys. Rev. Lett.* **80**, 2027 (1998).
- [7] T. Weber, J. Herbig, M. Mark, H.-C. Ngerl, and R. Grimm, *Science* **299**, 232 (2003).
- [8] L. Viverit, S. Giorgini, L. P. Pitaevskii, and S. Stringari, *Phys. Rev. A* **63**, 033603 (2001).
- [9] N. Chamel and P. Haensel, *Living Rev. Relativity* **11**, 10 (2008).
- [10] E. Wigner and F. Seitz, *Physical Review* **46**, 509 (1934).
- [11] N. Chamel, S. Naimi, E. Khan, and J. Margueron, *Physical Review C* **75**, 55806 (2007).
- [12] A. Bulgac and Y. Yu, *Phys. Rev. Lett.* **88**, 042504 (2002).
- [13] M. Grasso and M. Urban, *Physical Review A* **68**, 033610 (2003).
- [14] G. Bruun, Y. Castin, R. Dum, and K. Burnett, *The European Physical Journal D-Atomic, Molecular, Optical and Plasma Physics* **7**, 433 (1999).
- [15] J. Margueron and E. Khan, *Phys. Rev. C* **86**, 065801 (2012).
- [16] A. Pastore, J. Margueron, P. Schuck, and X. Viñas, *Phys. Rev. C* **88**, 034314 (2013).
- [17] A. Pastore, F. Barranco, R. A. BrogliA, and E. Vigezzi, *Phys. Rev. C* **78**, 024315 (2008).
- [18] A. Bulgac, *Physical Review C* **65**, 051305(R) (2002).
- [19] P. J. Borycki, J. Dobaczewski, W. Nazarewicz, and M. V. Stoitsov, *Phys. Rev. C* **73**, 044319 (2006).
- [20] D. C. Ralph, C. T. Black, and M. Tinkham, *Phys. Rev. Lett.* **74**, 3241 (1995).
- [21] P. Schuck and K. Taruishi, *Physics Letters B* **385**, 12 (1996), ISSN 0370-2693.
- [22] M. A. Baranov, *Pis'ma v ZhETF* **70**, 392 (1999).
- [23] G. Bruun and H. Heiselberg, *Physical Review A* **65**, 053407 (2002).
- [24] A. Schirotzek, Y.-i. Shin, C. H. Schunck, and W. Ketterle, *Phys. Rev. Lett.* **101**, 140403 (2008).
- [25] F. Serwane, G. Zürn, T. Lompe, T. Ottenstein, A. Wenz, and S. Jochim, *Science* **332**, 336 (2011).
- [26] D. Ralph, C. Black, and M. Tinkham, *Physical review letters* **74**, 3241 (1995).
- [27] M. Farine, P. Schuck, and X. Viñas, *Phys. Rev. A* **62**, 013608 (2000).
- [28] M. Urban and P. Schuck, *Phys. Rev. A* **67**, 033611 (2003).
- [29] M. Grasso, E. Khan, and M. Urban, *Phys. Rev. A* **72**, 043617 (2005).